

EXPERIMENTAL AND NUMERICAL EVALUATION OF A STEAMLINE BEHAVIOUR USING LOCAL APPROACH

Received - Primljeno: 2006-04-11

Accepted - Prihvaćeno: 2006-09-30

Original Scientific Paper - Izvorni znanstveni rad

Results of the experimental and numerical comparative analysis of steamline pipes have been presented. New pipes and the pipes used for more than 117,000 hours at 540 °C under pressure of 42 bars have been simultaneously tested. This testing has been carried out because frequent failures of the equipment components exposed to elevated temperatures, such as steam pipelines, make it necessary to pay particular attention to the analysis of the materials used. The most frequent failures were those connected with occurrence of cracks, particularly expressed in case of steel 14MoV6 3. Local approach to fracture has been developed for complete understanding of fracture mechanism. This approach combines theoretical, experimental and numerical solutions.

Key words: *local approach to fracture, 14MoV6 3 steel, notched tensile specimen, ductile fracture, FEM calculation*

Eksperimentalna i numerička ocjena ponašanja parovoda primenom lokalnog pristupa. Prikazani su rezultati usporednih, eksperimentalnih i numeričkih ispitivanja cijevi parovoda. Usporedno su ispitivane nove cijevi i cijevi koje su bile 117 000 sati izložene tlaku od 42 bara na temperaturi od 540 °C. Ovo ispitivanje je sprovedeno zbog učestalih otkaza dijelova opreme izloženih povišenim temperaturama, kao što je slučaj s cijevima parovoda. Zbog toga je bilo neophodno posvetiti posebnu pozornost ispitivanju materijala za izradu parovoda. Najčešći otkazi se manifestuju pojavom pukotina, posebno u slučaju čelika 14MoV6 3. Lokalni pristup mehanike loma je razvijen u cilju potpunog opisa mehanizma loma. On predstavlja kombinaciju teorijskih, eksperimentalnih i numeričkih rješenja.

Ključne riječi: *lokalni pristup mehanike loma, čelik 14MoV6 3, vlačne epruvete s utorom, plastični lom, proračun (FEM) MKE*

INTRODUCTION

The development of 14MoV6 3 steel (DIN) for highly loaded steam pipelines in late seventies offered significant benefits compared to the steels of previous generations [1, 2]. It was very popular for steam lines design and construction due to increased steam parameters (temperature up to 540 °C and pressure as high 45 bar for service life of 117,000 operating hours), allowing reduced wall thickness of pipes.

However, frequent premature failures of steam lines produced of this steel, in some cases only after 30,000 service hours, imposed the requirement for retrofit of damaged steam pipelines. Typical examples are steam lines of thermoelectrical power plants in Greece [3] and

in Germany [4]. This unexpected repair cost caused the application of 14MoV6 3 steel ambiguous and the designers prefer to replace it by other, highly alloyed steels (e.g. alloyed steel X12 CrMoV 1, according DIN, low alloyed steel 10CrMo9) for higher steam parameters. There is no clear explanation for failure occurrence, and steel producers claim that steel 14MoV6 3 is suited for the intended application [2]. Better understanding of in-service behaviour of 14MoV6 3 steel can help in reducing forced shutdowns and to improve the reliability and service safety of thermoelectric power plants.

BRIEF THEORETICAL OVERVIEW

Local or micromechanical approach to fracture has been developed for better understanding of fracture mechanism, including the material degradation process. This approach combines theoretical, experimental and numerical methods enables a less conservative assessment

M. Zrilić, M. Rakin, Lj. Milović, Faculty of Technology and Metallurgy University of Belgrade, Belgrade, Serbia, Z. Burzić, V. Grabulov, Military Technical Institute, Belgrade, Serbia

in structural integrity. Originally developed for predicting the toughness of steel for pressure vessels in nuclear plants and subsequently employed in steel industry, it has been recently used to explain the fracture mechanisms in heterogeneous material [1 - 4]. It was developed for ductile and cleavage damage processes, and lately the phenomena related to the field of transition temperatures have been investigated using that approach.

The process of ductile damage is developed through three stages: void nucleation, their growth and finally void coalescence resulting in material failure [5]. Voids are formed during material loading under critical normal stress at the boundary inclusion surface and grain boundaries particularly triple point. The next stage in ductile fracture development is the growth of voids and it is considered as most important. Growth of nucleated voids is strongly dependent on stress and strain state. Most of experiments and analyses show an exponential increase with the stress triaxiality, defined as the ratio of the mean stress σ_m and equivalent stress σ_{eq} . Increase of external loading affects further growth of voids and their eventual coalescence.

According to uncoupled modeling, void presence does not significantly alter the behaviour of the material [6], so that the damage parameter is not represented in the yield criterion. Major advantage of that approach may be simple numerical procedure and possibility to use the results of a single FE calculation for many postprocessing routines. Here, frequently applied uncoupled model of Rice and Tracey [7] is used. According to the model, growth of an isolated void in remote uniform Von Mises plastic field is given as:

$$\ln\left(\frac{R}{R_0}\right) = \int 0,283 e^{\frac{3\sigma_m}{2\sigma_{eq}}} \cdot d\varepsilon_{eq}^p, \quad (1)$$

where:

R - stands for the actual mean void radius,
 R_0 - its initial value then R/R_0 void growth ratio,
 σ_m/σ_{eq} - represents stress state triaxiality, and
 $d\varepsilon_{eq}^p$ - the equivalent plastic strain increment.

This local criterion has been given by Beremin [8]:

$$\frac{R}{R_0} \geq \left(\frac{R}{R_0}\right)_c. \quad (2)$$

Void growth rate can be determined integrating right side from initial value of equivalent deformation to its actual value $d\varepsilon_{eq}^p$, for any point where σ_m and σ_{eq} are computed. The ratio σ_m/σ_{eq} represents stress triaxiality.

A question may arise about the consideration of the growth of an isolated void in a material that may contain

rather large number of voids, particularly in final stage of ductile fracture. Coupled approach to the material damage and ductile fracture initiation considers alloy as a porous medium where the influence of nucleated voids on the stress/strain state and plastic flow cannot be avoided. Here, the model proposed by Gurson, Tvergaard and Needleman is used, see [9, 10]. The void volume fraction f as variable is introduced into expression for plastic potential:

$$\phi = \frac{3\sigma'_{ij}\sigma'_{ij}}{2\sigma^2} + 2q_1 f \cosh\left(\frac{3q_2\sigma_m}{2\sigma}\right) - [1 + (q_1 f)^2] = 0, \quad (3)$$

where:

σ - denotes actual yield stress of the matrix of the material,
 σ'_{ij} - the stress deviator,
 q_1, q_2 - constitutive parameters.

EXPERIMENTAL PART

The chemical composition for both steels is given in Table 1. Designation "N" is used for new (virgin) 14MoV6 3 steel, designation "O" is used for old (used) steel. Chemical composition of both materials is in accordance with the standard-anticipated material (DIN 17175).

Table 1. Chemical Composition of 14MoV6 3 steel (mass %)
 Tablica 1. Kemijski sastav čelika 14MoV6 3 izražen u mas. %

	C	Si	Mn	P
DIN 17175	0,10-0,18	0,15-0,35	0,30-0,60	0,040 max
Used steel	0,13	0,20	0,36	0,014
New steel	0,12	0,21	0,36	0,013
	S	Cr	Mo	V
DIN 17175	0,040 max	0,30-0,60	0,50-0,65	0,25-0,35
Used steel	0,021	0,55	0,51	0,28
New steel	0,019	0,66	0,49	0,31

Microstructural observations of tested steels were carried out in order to determine the level of degradation of the old material. The samples were taken from various parts of the pipes; preparation of the specimens included fine grinding, polishing and etching with 3 % nital.

It appeared that the largest differences in the micro structures of the old and new material were detected on the outer surface of the pipes, thus the following analysis of the material degradation during exploitation will be presented on the micro structures of the outer pipe surface. The micro structure of the new material is bainitic, which is described in detail in [11] characterized by non-homogeneous grain size. The grains are of irregular shape and complex geometry, with a large number of grain boundaries

(Figure 1.). In the structure of the old material, increase of the grains as a result of the mechanism of integration is

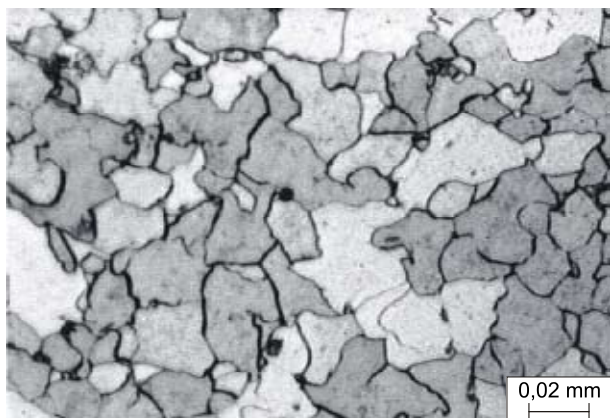


Figure 1. **Microstructure of new steel**
Slika 1. **Mikrostruktura novog čelika**

observed. Also, one can see a certain amount of voids at sulphides and particularly at second-phase particles (Figure 2.). The details of microstructure observations are given in [12, 13]. According to these results, ductile damage mechanism is dominant.

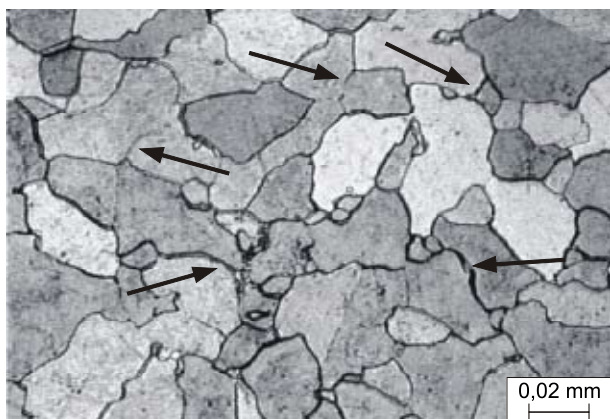


Figure 2. **Microstructure of used steel**
Slika 2. **Mikrostruktura rabljenog čelika**

Here care should be taken about the part of a micro structure for sampling, too. Namely, in this work only specimens cut from the flat parts of the steam pipelines have been analyzed. The intention was to make an effort to describe the level of damage using a simple model for ductile fracture, having in mind above specified microstructural observations. It is well known that the parts of the steam pipelines where the change of direction occurs are those subjected to maximum loading (e.g. elbows) and that, before making a decision on the model of local approach to be applied and necessity of taking into consideration creep of material, it is obligatory to make a microstructural analysis of steel at that part.

The samples of 14MoV6 3 steel were taken from new pipe and used pipes - withdrawn from service because of detected serious damage in several elbows and welded joints. The following specimens (Figure 3.), had been taken from pipe samples: tensile testing - ST; impact toughness testing - FT; local approach to fracture testing, with notch root radius 2 mm - NT2, 4 mm - NT4 and 10 mm - NT10; J -integral fracture toughness testing - SE(B) and da/dN - fatigue crack propagation assessment - FT.

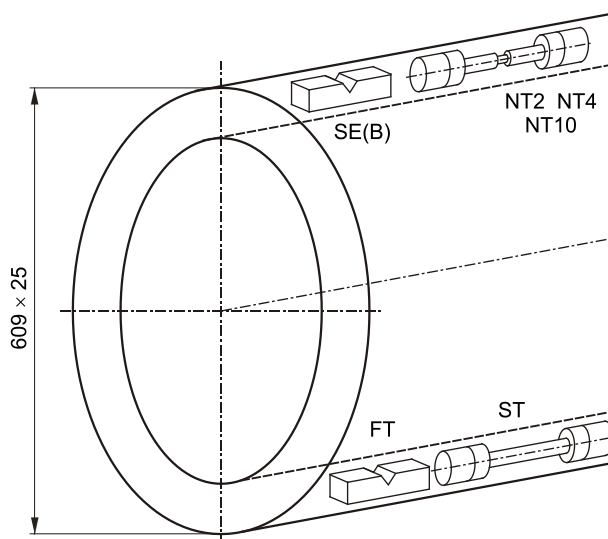


Figure 3. **Positions of specimens taken from new and used pipes**
Slika 3. **Raspored uzorkovanja epruveta iz novog i rabljenog materijala**

Here, the results of Charpy test and results representing methods of local approach to fracture are presented. The crack growth behaviour was analysed in [12].

Tensile properties of new and used 14MoV6 3 steels are determined by smooth standard specimens testing. Testing temperatures are 150 °C and 250 °C, and have been selected as appropriate for local approach testing and as basic data for J -integral determination. Steels of this class have similar values of tensile properties in the range from room temperature up to 150 °C. Higher temperature of 250 °C is selected for plastic analysis and pure ductile fracture for local approach to fracture.

The values of tensile properties are given in Table 2. Long-term exposure to elevated temperature under operating stresses affects the tensile properties of tested steel. This is expressed more in the yield stress than in tensile strength.

At higher testing temperature (250 °C), the difference between yield stress and ultimate tensile strength is more expressed. The reduction in elongation is of the same level at both testing temperatures. In general, tensile properties of used steel were still not critical regarding next service in exploitation.

Table 2. Mechanical properties of new (virgin) and used (old) 14MoV63 steel at 150 °C and 250 °C

Tablica 2. Mehanička svojstva novog i rabljenog čelika 14MoV63 na 150 °C i 250 °C

Steel	Temp / °C	Tens. strength R_m / MPa	Yield strength R_e / MPa	Long. elong ϵ_1 / %	Dia. elong ϵ_d / %
new	150	490	338	20,6	44,8
used	150	435	264	17,8	40,9
new	250	480	318	21,0	46,7
used	250	415	227	18,5	42,7

The impact toughness is almost the same for virgin and used steel when tested at 150 °C. Reduction in impact energy at room temperature is expressed only in crack propagation energy, not in crack initiation energy (see Table 3). As in the case of tensile properties, the reduction in impact toughness is not critical.

Table 3. Impact notch toughness of new (N) and used-old (O) 14MoV63 steels

Tablica 3. Energija loma zarezanih epruveta novog (N) i rabljenog (O) čelika 14MoV63

Spec.	Testing temper. / °C	Energy		
		total E / J	crack init. E_i / J	crack propag. E_p / J
N-1	20	193	74	119
N-2	20	148	72	76
O-1	20	102	66	36
O-2	20	102	77	25
N-1	150	230	67	163
N-2	150	241	64	177
N-3	150	227	57	170
O-1	150	235	65	170
O-2	150	235	68	167
O-3	150	216	54	162

Design of tensile specimen for experimental and numerical analysis is given in Figure 2. Specimens are produced with notch radius $R = 10; 4$ and 2 mm, according to [10]. In this way triaxiality effect is taken into account. By testing at elevated temperature, (here at 250 °C), pure ductile fracture occurred, Strain parameter in this case is reduction of the diameter in specimen notch root.

In Figure 5., records of load vs. diameter reduction for tested steels are shown. The reduction of plasticity of old steel is visible. Also, one can see that for the highest stress triaxiality (notch radius 2 mm), the largest difference between curves representing new (N) and old (O) material is obtained.

In order to determine void growth rate R/R_0 according to Eq. (1), for ductile fracture parameters calculation, “average

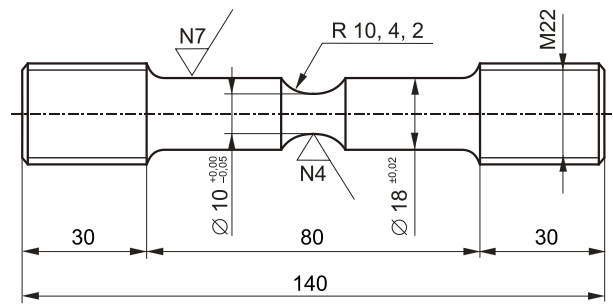


Figure 4. Geometry of notched tensile specimens for local approach to fracture analysis

Slika 4. Geometrija epruveta za vlak s utorom za analizu loma lokalnim pristupom

fracture strain” $\bar{\epsilon}_F$ and “average fracture strain” $\bar{\sigma}_F$ values are computed:

$$\bar{\epsilon}_F = 2 \ln \left(\frac{d_0}{d_F} \right) \quad (4)$$

and

$$\bar{\sigma}_F = \frac{4 \cdot F_F}{\pi \cdot d_F^2}, \quad (5)$$

according to [14].

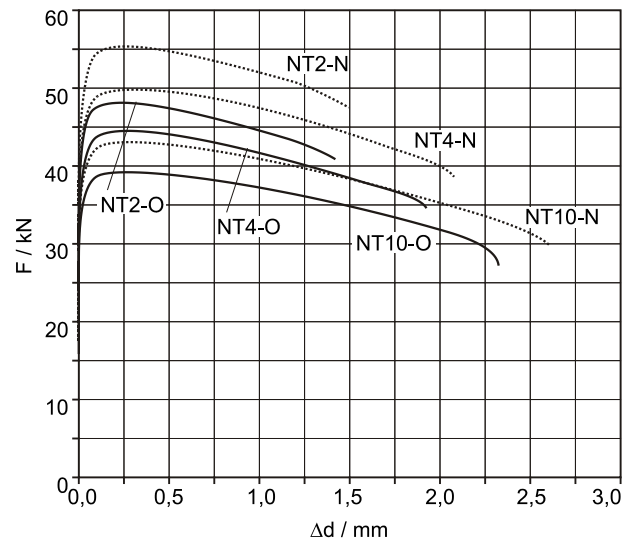


Figure 5. Load (F) vs. contraction of notch root diameter (Δd), for new (N) and used (O) steel, with notch radius 2 mm (NT2), 4 mm (NT4) and 10 mm (NT10)

Slika 5. Sila (F) - suženje u zoni utora (Δd), za novi (N) i rabljeni (O) čelik, s polumjerom utora 2 mm (NT2), 4 mm (NT4) i 10 mm (NT10)

The initial value of diameter in root radius, d_0 , and its final value, d_F , as well as fracture load, F_F , can be obtained experimentally, in tensile testing of notched round specimens, see Figure 6.

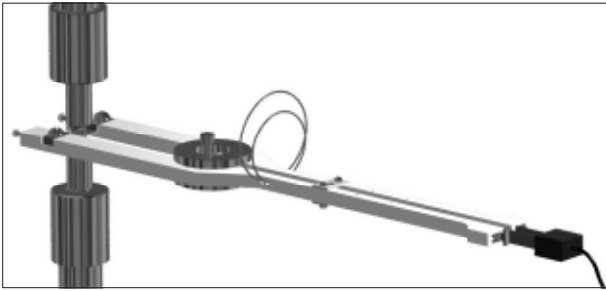


Figure 6. Design of diametric extensometer (measuring range 10 mm, accuracy 0,01%, applicable up to the temperature +600 °C)

Slika 6. Konstrukcija ekstenzometra za mjerenje suženja (mjerni opseg 10 mm, točnost 0,01 %, za temperature do + 600 °C)

The calculation is carried out using a post-processing program (details are given in [14]). The void growth ratio R/R_0 is calculated in each mesh element using Eq (1). The critical value, $(R/R_0)_c$, is computed at the place of maximum void growth ratio governed by stress triaxiality, σ_m/σ_{eq} , where σ_m represents mean stress and σ_{eq} Von Mises equivalent stress. Condition that should be fulfilled is agreement between experimentally and numerically obtained curves for tested geometries.

For the notched specimens tested here, the place where crack initiated is the specimen center, Figure 7. At that place $(R/R_0)_c$ is determined. Finite elements (FE) calculation is performed by elastic-plastic analysis in NASTRAN

software, using 3D elements. Upper specimen half is modeled as a wedge element, with angle of 5°, corresponding to 1/72 part of upper specimen part. This affects the shape of finite elements mesh, producing wedge type elements around axes, and the other elements are of brick type.

Also, void growth ratio is computed at maximum load, $(R/R_0)_m$, as a parameter representing damage due to ductile fracture before the final rupture of the specimen.

Five specimens were tested for each geometry in order to determine the critical void growth ratio, $(R/R_0)_c$ and void growth ratio corresponding to ultimate tensile strength, $(R/R_0)_m$, of new and used steel. In Table 4., average values are shown (N - new steel, O - old steel) for three geometries

Table 4. Critical void growth ratio (for final rupture) $(R/R_0)_c$ and at maximum load, $(R/R_0)_m$

Tablica 4. Rast šupljine (za trenutak loma) $(R/R_0)_c$ i maksimalnu silu, $(R/R_0)_m$

Spec.	Average values for 5 tested specimens			
	$\ln(R/R_0)_c$	$\ln(R/R_0)_m$	$\ln(R/R_0)_c$	$\ln(R/R_0)_m$
10N	0,6136	0,0792	1,8470	1,0824
4N	0,5467	0,0751	1,7275	1,0780
2N	0,3790	0,0659	1,4609	1,0682
10O	0,5612	0,0742	1,7670	1,0770
4O	0,4855	0,0702	1,6250	1,0727
2O	0,3112	0,0621	1,3650	1,0641

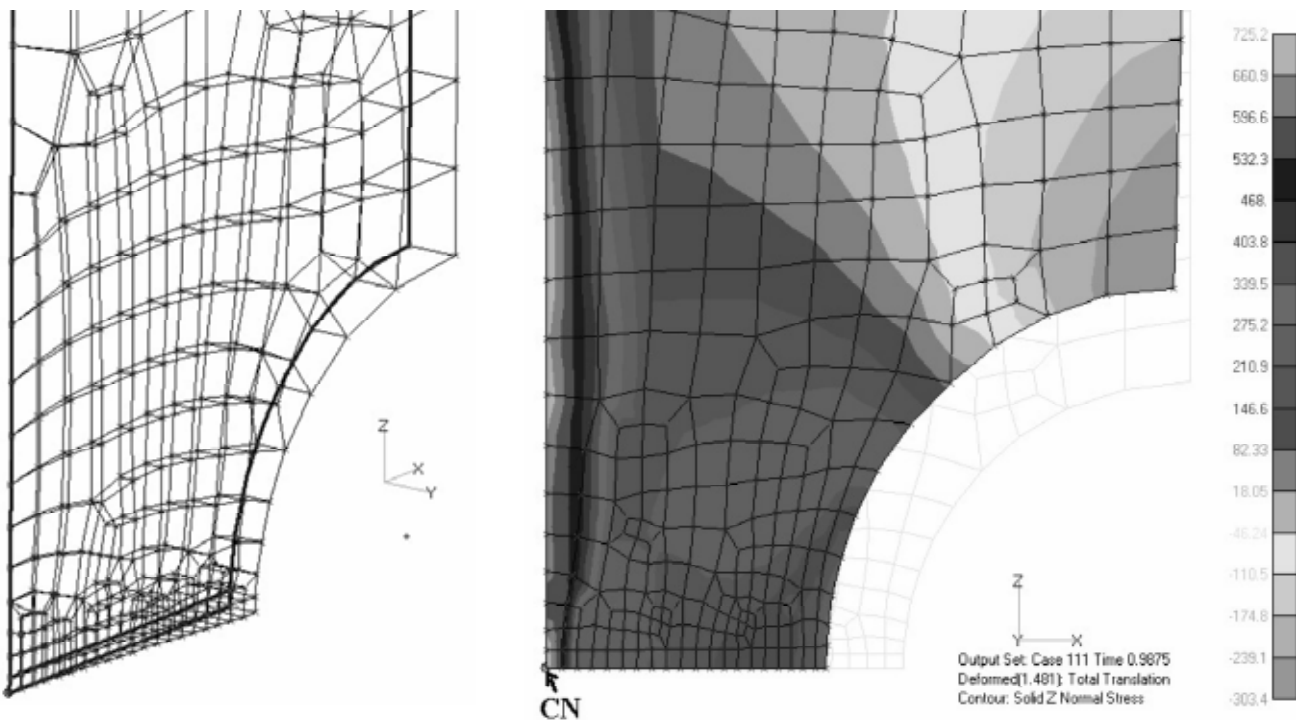


Figure 7. Notched tensile specimen mesh for notch root radius $R = 4$ mm (left), stress distribution for notch root radius $R = 4$ mm (right), [12]

Slika 7. Epruveta s utorom za vlak s polumjerom utora $R = 4$ mm (lijevo), raspodjela napreznaja za polumjer utora $R = 4$ mm (desno), [12]

of notched specimens: notch root radius 10 mm; 4 mm and 2 mm. Taking into account that a difference between computed values of void growth ratio is small, and almost independent of notch radius, final average values are determined for new and used material (see Table 5.).

Table 5. Average values of void growth ratio (critical and for maximum load) for analysed geometries
Tablica 5. Srednje vrijednosti rasta šupljine (kritične i za maksimalnu silu) za ispitivane geometrije epruveta

Spec.	Final average values			
	$\ln(R/R_0)_c$	$\ln(R/R_0)_m$	$(R/R_0)_c$	$(R/R_0)_m$
10N				
4N	0,5131	0,0734	1,68	1,08
2N				
10O				
4O	0,4526	0,0688	1,59	1,07
2O				

In Table 6. reduction percentage of void growth ratio R/R_0 is presented for the final fracture and at maximum load values. The comparison of local approach parameter defining the level of damage of the material, at adopted temperature, can be expressed via the critical value $(R/R_0)_c$ and value corresponding to tensile strength, $(R/R_0)_m$.

Table 6. Decrease of values of void growth ratio (critical and for maximum load) for used steel
Tablica 6. Smanjenje rasta šupljine (kritične i za maksimalnu silu) za rabljeni čelik

$(R/R_0)_c / \%$	$(R/R_0)_m / \%$	$*(R/R_0)_c - 1 / \%$	$*(R/R_0)_m - 1 / \%$
5,5	0,5	13,7	6,5
*normalized void growth (due to log scale)			

Micromechanism of fracture is ductile, as shown on Figures 8.a and 8.b, indicated by nucleation of voids on particles (large particles are assumed to be inclusions and small particles are assumed to be carbides), their growth by decohesion and further coalescence. This behaviour, established using SEM, has verified local approach to

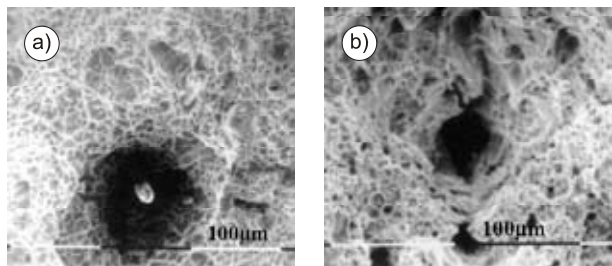


Figure 8. SEM pictures of fracture surface on notched specimens, $R = 10$ mm; a) new steel and b) old steel
Slika 8. SEM fotografija površine loma epruvete s utorom, $R = 10$ mm; a) novi čelik i b) rabljeni čelik

ductile fracture, since in both cases the mechanism is purely ductile, without characteristics of brittle fracture on fractured surface.

CONCLUSIONS

The agreement of experimental and numerical analysis of notched tensile specimens, is the basic condition for calculation of local criterion for ductile fracture. In this way material's characteristics, precisely describing material properties, are available for modern computational methods, such as FEM.

Described properties of local approach to fracture enabled more precise evaluation of degradation of steel 14MoV6 3 properties after long-term exposure to elevated temperature. An obtained result indicates that critical void growth rate is improved by 13,7 %, while void growth at maximum load is improved by 6,5 %. This is attributed to difference in inter carbide distance, due to coarsening.

It is possible to conclude that considered steel can be further used in exploitation, although specified service life is spent. However, prescribed proper in-service inspection is obligate. In that way, the economical benefit could be significant. Further development in local approach to fracture requires more efforts, particularly on inhomogeneous structures such are welded joints.

REFERENCES

- [1] H. Kaes: Erfahrungen mit dem Stahl 14MoV6 3, Bericht des VGB-Ausschusses für Materialfragen, Essen, 1966.
- [2] W. Arnswald, H. Kaes: Verwendung des Stahles 14MoV6 3 für Rohrleitungen, VGB Konferenz, 1985, p. 356.
- [3] H. Kessler, W. Hoppe: Teilaustausch von HD- und HZU- Leitungen in einem 2×300 MW in Griechenland, Lebensdauer von Rohrleitungen in Kraftwerken, Mannesmann Anlagebau AD, Dusseldorf, 1987, p. 373.
- [4] H. Lesper, H. Mayer, H. Hennecke, W. Laughardt, H. Musch: Austausch von FD- und HZE-Leitungen im VEW Kraftwerk Westfalen, Lebensdauer von Rohrleitungen in Kraftwerken, Mannesmann Anlagebau AD, Dusseldorf, 1987, p. 345.
- [5] P. F. Thomason: Ductile Fracture of Metals, Pergamon Press, 1990.
- [6] L. Bauvineau et al.: Modelling ductile stable crack growth in a C-Mn steel with local app, Proc. Eurom-Mecamat Conf. Loc. App. Fract., Fontainebleau, 1996, p. 22 - 32.
- [7] J. R. Rice and D. M. Tracey: On the ductile enlargement of voids in triaxial stress fields. J. Mech. Phys. Solids 17 (1969), 201 - 217.
- [8] F. M. Beremin, 5th International Conference of Fracture, Pergamon Press, 1981[1].
- [9] A. L. Gurson. Continuum theory of ductile rupture by void nucleation and growth: Part I. J. Eng. Mat. Techn. 99 (1977), 2 - 15.
- [10] V. Tvergaard and A. Needleman: Analysis of cupe-cone fracture in round tensile bar. Acta Metall. 32 (1984), 157 - 169.
- [11] B. Walsler, A. Rosselet, VGB Kraftwerkstechnik 58 (1978), 361.
- [12] M. Zrilic: The Application of Local Approach to Residual Life Assessment of Equipment Components at Elevated Temp. Ph.D. Thesis (in Serbian) Fac. of Techn. Metall. Belgrade, 2004.
- [13] M. Zrilic et al.: Ductile fracture prediction of steam pipeline steel, Mat. Sci. Forum 495 (2006), 537 - 542.
- [14]ESIS P6-98: Procedure to measure and calculate material parameters for the local approach to fracture using notched tensile specimens, European Structural Integrity Society (ESIS), 1998.